# NONLINEAR MODEL PREDICTIVE CONTROL FOR
# THE ALSTOM GASIFIER BENCHMARK PROBLEM

**R. K. Al Seyab   and   Y. Cao** [1]

*School of Engineering, Cranfield University, UK*

Abstract: Model predictive control has become a first choice control strategy in industry because it is intuitive and can explicitly handle MIMO linear and nonlinear systems with the presence of variable constraints and interactions. In this work a nonlinear state-space model has been developed and used as the internal model in predictive control for the ALSTOM gasifier. A linear model of the plant at 0% load is adopted as a base model for prediction. Secondly, a static nonlinear neural network model has been created for a particular output channel, fuel gas pressure, to compensate its strong nonlinear behaviour observed in open-loop simulation. By linearizing the neural network model at each sampling time, the static nonlinear model provides certain adaptation to the linear base model. Noticeable performance improvement is observed when compared with pure linear model based predictive control. *Copyright © 2005 IFAC*

Keywords: Predictive control, Gasification, Neural network, Linearization.

## 1. INTRODUCTION

A gasifier is essentially a chemical reactor where coal reacts with air and steam to produce low calorific value fuel gas, which then can be burnt in a suitably adapted gas turbine. In modern advanced power generating plants, gasification helps burning coal in a new and environmentally clean process.

Based on an industrial scale gasifier, the ALSTOM Power Technology Centre issued a benchmark challenge in 1997 and a second round challenge in 2002. The first round challenge included three linear models representing three operating conditions of the gasifier at 0%, 50% and 100% load respectively. The challenge requires the controller to control the gasifier at three load conditions to satisfy input and output constraints in the presence of step and sinusoidal disturbances. (see Dixon et al (2002)). An overview and comparison of various control approaches submitted to the first round challenge are given in (Dixon 1999).

None of the proposed controllers managed to meet all the performance criteria while satisfying the specified constraints. The only model predictive control (MPC) approach proposed to the first round challenge by Rice et al (2002) involved the use of a linear MPC with an additional inner loop to stabilize the process. The inner loop controller is supervised by an outer loop to handle the process constraints.

The second round of the challenge issued in 2002 extended the original problem by providing participants with a nonlinear simulation model of the gasifier in MATLAB\SIMULINK (Dixon 2002). In addition to the original disturbance test, two extra tests: load change and coal quality disturbance tests were included. Recently, a group of control solutions for the benchmark problem were presented at Control-2004 at Bath University, UK in September 2004. Most of controllers were reported as capable to control the system at disturbance and load change tests. This was not the case for the coal quality disturbance test because of the char flow rate saturation behaviour. In the previous work (Al Seyab et al 2004) a linear MPC employing Generalized Predictive Control (GPC) strategy was proposed. The operating condition at 0% load point was

considered to be the worst case and a linearized model around this load condition was adopted for the internal model. The controller was able to attain all the required performance specifications within the input and output constraints at all load conditions. In this work, it is shown that the plant/model mismatch can be further reduced using a partially developed nonlinear model instead of a pure linear model. More specifically, a nonlinear neural network model is developed for a static single output channel, fuel gas pressure (PGAS) to compensate for its strong nonlinear behaviour observed in open loop simulation. The nonlinear model was then linearized at every sampling instance to provide adaptation to the main linear controller. A similar strategy can be used for the other output variables but this was found neither necessary nor very productive. The partial nonlinearity compensated model leads to considerable performance improvement. The rest of this paper is organized as follows. Section 2 includes a short description of the ALSTOM gasifier benchmark problem. The details of the MPC algorithm and the internal model are discussed in section 3. Section 4 explains the procedures of nonlinear system identification and controller design. Section 5 presents the simulation results, and in section 6 some conclusions are drawn from this work.

## 2. SYSTEM DISCRPITION

The ALSTOM gasifier is a $(5 \times 4)$ MIMO nonlinear plant. One of the inputs, limestone mass (WLS) is used to absorb sulphur in the coal and its flow rate must be set to a fixed ratio of 1:10 against another input (WCOL) . This leaves effectively 4 degrees of freedom for the control design. The plant inputs and outputs with their limits are given in Table 1. The full model of the gasifier has 25 states and the aim of the benchmark challenge is to design a controller to work with the given SIMULINK model as the plant to satisfy the control performance. The control specification includes sink pressure step and sine wave disturbance testes (at the three different operating points), load ramp change from 50% to 100%, and coal quality change by $\pm 18\%$. The specifications of these tests that must be met are given in details in (Dixon 2002).

## 3. INETRNAL MODEL DISCRPITION

Linear models with linear constraints and quadratic objective function result in convex optimization problems easily solved using Quadratic Program-ming (QP). To extend linear MPC to the control of nonlinear processes, a model is required that can represent the salient nonlinearities but possibly without the complication associated with general nonlinear models. Wiener model corresponds to a plant with linear dynamics but nonlinear static gain and can adequately represent many of nonlinearities commonly encountered in industrial processes (Sandra et al 1998, Dumont et al 1994).

Table 1 Outputs and inputs variables and limits

| Outputs | Description | Allowed fluctuations |
|---|---|---|
| CVGAS | Fuel gas calorific value | $\pm$ 0.01 MJ/kg |
| MASS | Bed mass | $\pm$ 500 kg |
| PGAS | Fuel gas pressure | $\pm$ 0.1 bar |
| TGAS | Fuel gas temperature | $\pm$ 1 K |

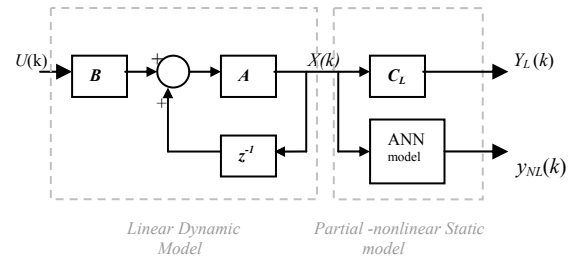| Inputs | Description | Maximum | Peak rate . |
|---|---|---|---|
| WCHR | Char extraction rate | 3.5 kg/s | 0.2 kg/s$^2$ |
| WAIR | Air flow rate | 20 kg/s | 1.0 kg/s$^2$ |
| WCOL | Coal flow rate | 10 kg/s | 0.2 kg/s$^2$ |
| WSTM | Steam flow rate | 6 kg/s | 1.0 kg/s$^2$ |



Fig.1. The nonlinear internal model.

In this work, the original linear MPC design (Al Seyab et al 2004) is extended to include some of the plant nonlinearities by developing a static nonlinear model in the form of Wiener configuration as shown in figure 1. Linear static gains are used for three outputs, CVGAS, MASS, TGAS, while, an artificial neural network (ANN) model is created for the forth output PGAS. The output selection was based on the open-loop step response comparison between the linear and nonlinear simulation model (see figure 2). The results showed that the linear model can correctly capture the dynamic behaviour in three of the four outputs for up to 20s (the practical prediction horizon length) under all load conditions. However, the forth output PGAS exhibits salient nonlinearities which cannot be predicted by the linear model. It is also observed that the effect of the unmeasured disturbance PSINK on the output variable PGAS is quite large, whilst the time constant of the response is very short compared to that of other outputs. Therefore, even for a short prediction horizon ($P \leq 20$s), both transient and static behaviour of PGAS should be covered by a prediction model, while for other outputs only transient characteristics have dominant response. Hence, a static nonlinear model would not be very useful for the other variables unless a very long prediction horizon (about $10^4$ s) is used which is clearly not practical.

Assuming that the plant has manipulated inputs, $\widetilde{u} \in \mathfrak{R}^{n_u}$ and outputs $\widetilde{y} \in \mathfrak{R}^{n_y}$, which have steady-state values, $\widetilde{u}_0$ and $\widetilde{y}_0$ at the nominal operating point, the partially nonlinear predictive model can be described by the following discrete time state-space model:

$$x(k+1) = A\,x(k) + B\,u(k)$$
$$y_L(k) = C_L x(k), \quad y_{NL} = f_{NN}(x(k)) \tag{1}$$

where $k$ stands for $kth$ sampling time, $u(k) = \tilde{u}(k) - \tilde{u}_0$ and $y(k) = \tilde{y}(k) - \tilde{y}_0$ are deviation variables. Outputs are divided into two groups: $y_L(k)$ outputs vector corresponding to the linear variables CVGAS, MASS, and TGAS, and $y_{NL}(k)$ corresponding to nonlinear output, PGAS. The vector $x(k)$ contains the internal states of the model. The matrix $C_L$ represents the linear static gain, while $f_{NN}$ is the nonlinear function modelled by a neural network. Initially, the plant is assumed to be at the nominal operating point with $x(0)=0$, $u(0)=0$, $y(0)=0$.

The matrices $A$, $B$, and $C_L$ are obtained by linearizing the nonlinear plant model at 0% load condition. The ANN static model consists of two hidden layers and one output layer. The hidden layers transfer function is the nonlinear function *Tansig–sigmoid* type while a linear transfer function is used for the output layer. The mathematical form of the function $f_{NN}$ is given in a vector form as :

$$H_1 = f_s(W_1 x(k) + b_1), \quad H_2 = f_s(W_2 H_1 + b_2),$$
$$y_{NL}(k) = W_3 H_2 + b_3 \tag{2}$$

where $H_1$, $H_2$ and $y_{NL}$ are the output values of each layer. The values $W_1$, $W_2$, and $W_3$ are the weight parameters while $b_1$, $b_2$, and $b_3$ are the bias parameters. The function $f_s(.)$ is the sigmoid tangent function which is defined as, $f_s(n) = (2/(2 + e^{-2n})) - 1$.

Because the model in equation 1 is nonlinear, the problem is no longer convex. In order to use efficient QP algorithm, local linearization of the static ANN model around the current states is required. Future predictions of output based on current measurement $y_{NL}(k)$ can be approximated by the first two terms of the Taylor series expansion:

$$y_{NL}(k+i) = n_k + C_{NL}x(k+i) \quad for\ i = 1,\dots,P \tag{3}$$

where, $\quad n_k = f_{NN}(x)\big|_{x=x(k)} - \dfrac{\partial f_{NN}(x)}{\partial x}\bigg|_{x=x(k)} x(k)$

and $\quad C_{NL} = \dfrac{\partial f_{NN}(x)}{\partial x}\bigg|_{x=x(k)}$

The partial derivative $\partial f_{NN}/\partial x$ can be calculated from the neural network structure in equation 2 using the chain rule as:

$$\frac{\partial f_{NN}}{\partial x} = W_3\ diag\ (I - H_2 H_2^T)W_2 \times \tag{4}$$
$$diag\ (I - H_1 H_1^T))W_1$$

This results in a time-varying linear state-space model to be used in predictive control.

## 4. PREDICTIVE CONTROL FORMULATION

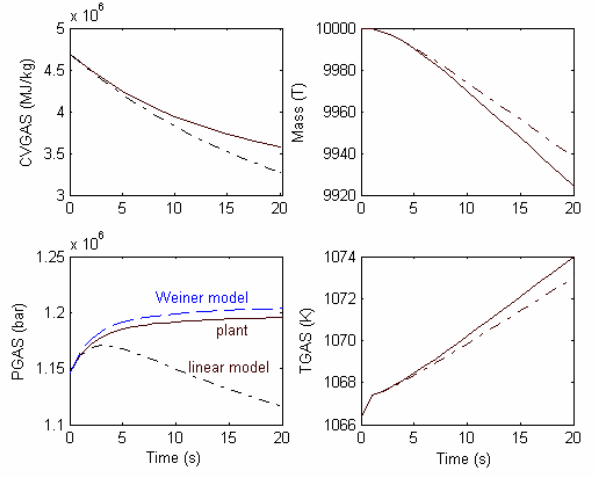The prediction model to be used can be represented by the following state-space equation:



Fig.2. Open-loop step response at 0% load condition.

$$x(k+1) = A x(k) + B u(k) \tag{5}$$
$$y(k) = Cx(k) + d(k)$$

where, $y(k) = \begin{bmatrix} y_L(k) & y_{NL}(k) \end{bmatrix}^T$, $C = \begin{bmatrix} C_L & C_{NL} \end{bmatrix}^T$, $d(k)$ is the virtual output disturbance estimated from the outputs measurement to reduce the plant-model mismatch. Note, $n_k$ in (3) is absorbed into $d(k)$. At the $k$th sampling time, with currently measured outputs, $y_m(k) = \tilde{y}(k) - \tilde{y}_0$, and the current states $x(k)$, the future output within the prediction horizon, $P$ can be estimated from the future input (to be determined within the moving horizon, $M$) $u(k)$ as follows. Taking

$$d(k+i) = d(k) = y_m(k) - Cx(k) \quad for\ i = 1,\dots,P,$$

then, $\quad Y = \Phi U + \Psi x(k) + L\,d(k) \tag{6}$

where, $Y = [y^T(k+1) \quad \cdots \quad y^T(k+P)]^T$
$\qquad U = [u^T(k) \quad \cdots \quad u^T(k+M-1)]^T$

$$\Phi = \begin{bmatrix} CB & 0 & \cdots & 0 \\ CAB & CB & \cdots & 0 \\ \vdots & \vdots & \cdots & 0 \\ CA^{P-1}B & CA^{P-2}B & \cdots & \sum_{i=M}^{P} CA^{P-i}B \end{bmatrix}, \Psi = \begin{bmatrix} CA \\ \vdots \\ CA^P \end{bmatrix},$$

and $\quad L = \begin{bmatrix} I \cdots I \end{bmatrix}^T$.

Future input, $U$ is determined so as to follow a reference, $r(k)$, *i.e.* to minimize the performance cost: $(Y - L\,r)^T Q\,(Y - L\,r)$ subject to input constraints, $\underline{u} \le u \le \bar{u}$, and input rate constraints, $u(k+1) - u(k) \le \sigma_u$. Using the predictive equation (6), a QP optimization problem is formulated.

$$\min_u J = 0.5\,U^T S\,U + U^T(X_1 x(k) - X_2(r_k - d_k)) \tag{7}$$

$$s.t. \qquad U \le \overline{U}, \quad -U \le \underline{U}$$
$$EU \le \Delta_u + F\,u(k-1), \quad -EU \le \Delta_u - F\,u(k-1)$$

where,
$u(k-1)$ is the previous input applied to the plant,

$$S = \Phi^T Q \Phi + R, \quad X_1 = \Phi^T Q \Psi, \quad X_2 = \Phi^T Q L$$

$$\overline{U} = [\overline{u}^T \cdots \overline{u}^T], \quad \underline{U} = [\underline{u}^T \cdots \underline{u}^T],$$

$$\Delta_u = [\sigma_u^T \cdots \sigma_u^T]$$

$$E = \begin{bmatrix} I & 0 & \cdots & 0 & 0 \\ -I & I & \cdots & \vdots & \vdots \\ \vdots & 0 & \cdots & \vdots & \vdots \end{bmatrix}, \text{ and } F = \begin{bmatrix} I & 0 & \cdots & 0 \end{bmatrix}^T$$

Note, the weighted input cost and the output constraints are ignored to simplify the controller with little effects on the performance. The only tuneable parameters in this formulation are *Q, P, M* and sampling time. Thus, the control strategy can be easily implemented and tuned to satisfy required performance. Only the first $n_u$ rows of the vector *U*, which corresponds to $u(k)$ are applied to the plant. The whole procedure is then repeated at the next sampling instance.

For the unconstraint case, the optimal solution, which corresponding to a state feedback control law, can be obtained analytically:

$$U = -K_1 x(k) + K_2(r_k - d_k) \qquad (8)$$
where $K_1 = S^{-1} X_1$ and $K_2 = S^{-1} X_2$

Let *K* be the first $n_u$ rows of $K_1$, then the nominal stability (perfect model without input saturation) of the closed-loop can be checked by calculating the eigenvalue of the matrix *A-BK*.

## 4. PREDICTIVE CONTROL DESIGN

### 4.1 Nonlinear System Identification.

The first design task to implement the above algorithm is to get an internal model using equation 5. Three operating conditions are specified in the gasifier benchmark problem: 0%, 50%, and 100% load conditions. Since the performance requirements at 50% and 100% load conditions are relatively easier to achieve, it was decided to use the 0% load point as the nominal point to get the linearized state space model. The model obtained was then reduced to 16 states via pole-zero cancellation. The 16 states model is discretized with the sampling time selected.

For the ANN static model of PGAS, the number of node in the first and second hidden layers was 16 and 10 respectively with one node in the output layer. Data were generated through applying a zero mean normalized sequence of random pulses with their periods and amplitudes corresponding to the maximum and minimum expected variations and frequency in response to individual input change under different load conditions. The sets over different loads were then linked together and used in training and validation of the ANN. The performance of the trained PGAS Wiener model is given in figure 2, which shows the model is capable to capture most characteristics behaviour of the plant.

### 4.2 Predictive control design.

Normally, the sampling time should be less than one tenth of $2\pi / \omega_b$, where $\omega_b$ is the required bandwidth of the closed-loop. The performance specifications require the imposition of a sine disturbance with a period of 25s (0.04 Hz). Therefore, the sampling time should be less than 2.5s. On the other hand, the sampling time should not be too large so that in any step disturbance test, the output variables will not deviate from their setpoints more than the limit specified before the controller starts to response. Hence, the sampling time was selected to be 1 s. This satisfies both requirements. The control algorithm is implemented in the form of a SIMULINK s-function to replace the control block in the nonlinear baseline model. The QP problem is solved by calling '*quadprog*' of the MATLAB/Optimization Toolbox at each sampling time. This is the major computation burden in the present algorithm and is solely determined by the length of the control horizon, *M*. The prediction horizon, *P* has little effect on computation burden, and thus can be select relatively large to improve robust stability. In this study, *M* = 7s and *P* = 17s. The weighting matrix, *Q* is diagonal and initially set to the inverse of the output error bounds. After online tuning, the final values were *Q* = $diag[1.0 \ 150 \ 3.0 \ 2 \times 10^6]$. Using the above configuration, nominal stability was achieved at all three load conditions. That is the magnitudes of all eigenvalues of $A_i - B_i K$ are less than 1. Where, $A_i$ and $B_i$ are the discrete state and control matrices at different load conditions.

## 5. SIMULATION RESULTS

### 5.1 Disturbance Tests.

The following two disturbance tests were performed for three load conditions for 300 seconds:
- Step change in sink pressure PSINK of -0.2 bar at t = 30 s.
- 0.04 Hz sinusoidal variation in PSINK of amplitude 0.2 bar beginning at t = 30 s.

All the results to follow are compared with the linear MPC. The maximum and minimum values as well as the peak rate change of the input variables of two disturbance tests under different load conditions are shown in Table 2. The maximum absolute error between output variables and their setpoints and the integral of absolute error (IAE) of these variables are calculated in Table 3 where (M1) and (M2) refer to the linear and nonlinear MPC approaches under comparison, respectively. The results are collected in tables to compare with other ALSTOM gasifer control approaches published before. Due to the space limitations only some plots of input and output responses are displayed here. Figures 3 to 5 show the system performance at 50% and 0% load conditions. In the 50% load case, the results are plotted for $t \leq 100s$ to present the control performance in more details. After this time period, all the outputs response remained constant. The results in Table 2 and 3 however are calculated until t=300s. For 0%

load sinusoidal test, results with extra simulation time are provided to confirm the satisfactory performance of output in meeting the given specifications. The results show that both controllers are capable of maintaining the output variables within the limits for the tests specified by ALSTOM. In the case of M2, an improvement in the whole system performance was observed. In fact, all output variables have benefited from using more accurate PGAS internal model. Due to multivariable interactions, the improvement in other output variables sometimes is even larger than that in PGAS itself (Figures 4 and 5). This is explained as follows. The response of PGAS, particularly to disturbance PSINK is much faster than other output variables (Figure 1). The Improvement of nonlinear model is mainly in long term prediction (Figure 1). Hence, it has more effect on slow-response variables rather than PGAS, which is a fast-response variable. Moreover, the maximum drop of PGAS in Figure 4 is the response to disturbance before the controller can take action, hence is not able to be reduced by changing internal model only.

### 5.2 Coal quality change test.

Both controllers M1 and M2 show a similar capability and they are capable to control the system under coal quality change at about $\pm 10\%$. This is not the case when the change increases to $\pm 18\%$ because the output TGAS deviates from the desired region after a cretin time. This divergence happened faster in the case of M2 controller at sine wave disturbance test at 0% load condition. This is a problem due to an inherent performance limitation. When the coal quality change is large, an input saturation of WCHR is unavoidable so that TGAS deviates a long way from the setpoint, i.e. temperature cannot be maintained at given setpoint without violating constraints of WCHR.

### 5.3 Load Change Test

In this test, the load is required to increase from 50% to 100% within time from 100 s to 700 s. The actual response is collected from the simulation and compared with the results when using M1 controller. For both controllers, good setpoint tracking performance is obtained. The outputs results show approximately similar behaviours for the two controllers, with a small improvement in the MASS response when using M2 approach. Also, the manipulated variables response is smoother in this case (see figures 6 -7).

### 6. CONCULSION

A simple predictive controller has been developed to control the ALSTOM gasifier benchmark process. LMPC employing GPC strategy is modified to include a partially nonlinear internal model. A nonlinear class Wiener model is used to identify one of the process output variables (PGAS) which has strong nonlinearity while a linear model at 0% load condition is adopted for the other output variables. To regain the convex feature of the QP optimization

problem, PGAS nonlinear model was linearized at every sampling time to update the linear model used for optimization. Thus, the internal model is actually a linear time-varying model. The new controller meets all the required performance specifications within given input and output constraints during sink pressure disturbance and load change tests and the results show a significant improvement in the system performance compared with the results obtained when only linear time-invariant model is used.
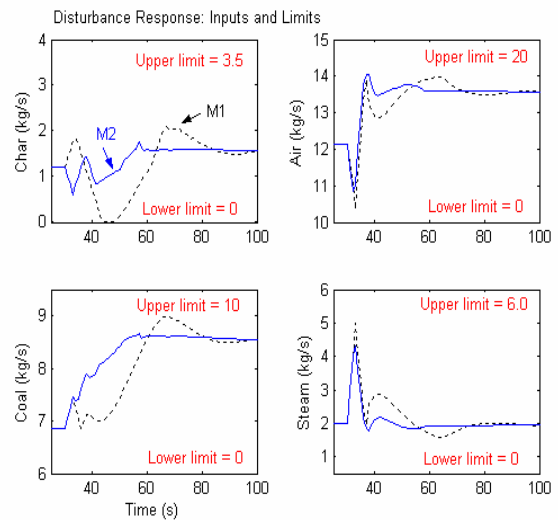


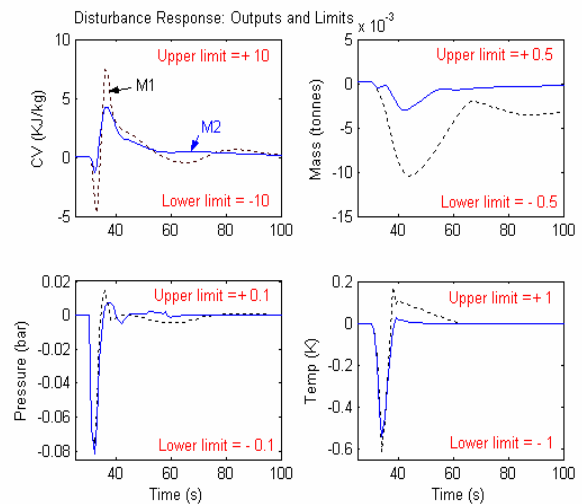Fig.3. Step disturbance: Inputs and limits at 50%.



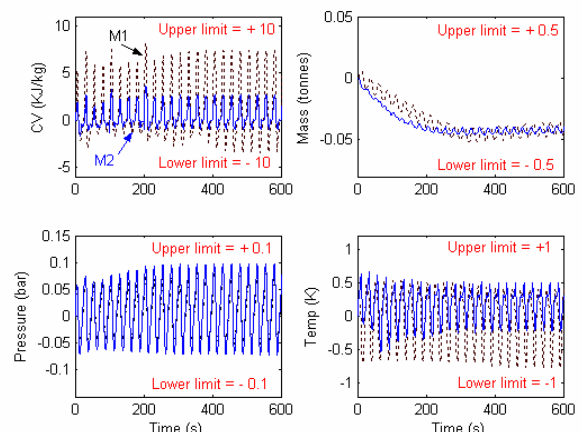Fig.4. Step disturbance: Outputs and limits at 50%.



Fig.5. Sine disturbance: Outputs and limits at 0%.

Table 2 Input results

| Step, 100% Load | Maximum M1 | M2 | Minimum M1 | M2 | Peak rate M1 | M2 |
|---|---|---|---|---|---|---|
| WCHR | 1.9005 | 1.3663 | 0 | 0.49026 | 0.2 | 0.2 |
| WAIR | 19.170 | 19.299 | 16.168 | 16.158 | 1.0 | 1.0 |
| WCOL | 10.00 | 10.00 | 8.5253 | 8.5542 | 0.2 | 0.2 |
| WSTM | 5.0793 | 4.7058 | 2.3046 | 2.3714 | 1.0 | 1.0 |
| Step, 50% | M1 | M2 | M1 | M2 | M1 | M2 |
| WCHR | 2.085 | 1.7589 | 0 | 0.5983 | 0.2 | 0.2 |
| WAIR | 13.99 | 14.062 | 10.354 | 10.85 | 1.0 | 1.0 |
| WCOL | 8.976 | 8.6559 | 6.8537 | 6.7943 | 0.2 | 0.2 |
| WSTM | 5.001 | 4.3151 | 1.5638 | 1.7889 | 1.0 | 1.0 |
| Step, 0% | M1 | M2 | M1 | M2 | M1 | M2 |
| WCHR | 2.1534 | 2.0469 | 0.2274 | 0.9532 | 0.2 | 0.2 |
| WAIR | 8.5508 | 8.7148 | 4.7147 | 4.781 | 1.0 | 1.0 |
| WCOL | 7.7216 | 7.6251 | 5.1574 | 5.1398 | 0.2 | 0.2 |
| WSTM | 4.2366 | 4.2366 | 1.0404 | 1.1511 | 1.0 | 1.0 |
| Sine, 100% | M1 | M2 | M1 | M2 | M1 | M2 |
| WCHR | 1.4640 | 1.725 | 0.3492 | 0.0742 | 0.2 | 0.2 |
| WAIR | 18.923 | 19.049 | 15.747 | 15.628 | 0.577 | 0.671 |
| WCOL | 9.7537 | 9.7444 | 7.2684 | 7.0443 | 0.2 | 0.2 |
| WSTM | 3.6452 | 3.7488 | 1.5192 | 1.5676 | 0.603 | 0.610 |
| Sine, 50% | M1 | M2 | M1 | M2 | M1 | M2 |
| WCHR | 1.9503 | 1.8531 | 0.11527 | 0.21605 | 0.2 | 0.2 |
| WAIR | 13.764 | 14.014 | 10.331 | 9.9657 | 0.623 | 0.7461 |
| WCOL | 8.1287 | 8.1573 | 7.2684 | 7.0443 | 0.2 | 0.2 |
| WSTM | 3.3492 | 3.548 | 0.6553 | 0.3868 | 0.678 | 0.5866 |
| Sine, 0% | M1 | M2 | M1 | M2 | M1 | M2 |
| WCHR | 2.3547 | 2.8559 | 0.12867 | 0 | 0.2 | 0.2 |
| WAIR | 8.905 | 8.9219 | 3.2579 | 3.4465 | 0.623 | 0.7461 |
| WCOL | 6.1213 | 6.4590 | 3.2334 | 2.860 | 0.2 | 0.2 |
| WSTM | 3.8088 | 4.3271 | 0 | 0 | 0.678 | 0.5866 |

Table 3 Output results

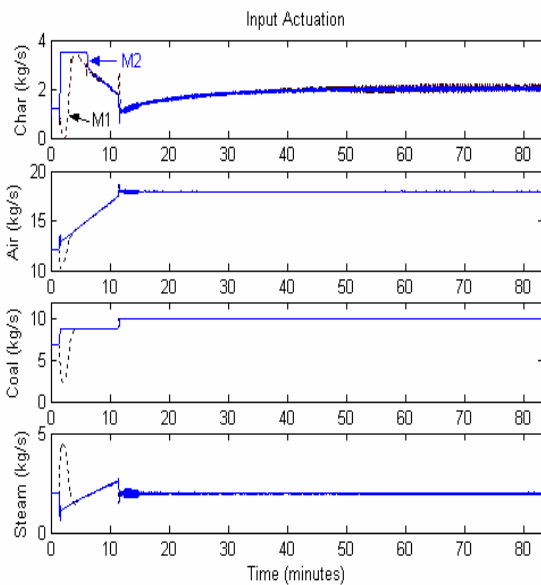| Step, 100% Load | Minimum absolute error M1 | M2 | Integral Absolutes Error M1 | M2 |
|---|---|---|---|---|
| CVGAS | 7.3762 | 5.6746 | 101.45 | 84.514 |
| MASS | 14.130 | 10.36 | - | - |
| PGAS | 0.06723 | 0.07399 | 0.28795 | 0.28386 |
| TGAS | 0.52016 | 0.51195 | - | - |
| Step, 50% | M1 | M2 | M1 | M2 |
| CVGAS | 7.4921 | 4.2407 | 85.186 | 66.793 |
| MASS | 10.615 | 3.239 | - | - |
| PGAS | 0.076128 | 0.08206 | 0.28795 | 0.34009 |
| TGAS | 0.61026 | 0.53916 | - | - |
| Step, 0% | M1 | M2 | M1 | M2 |
| CVGAS | 9.0048 | 2.5465 | 79.033 | 48.441 |
| MASS | 13.666 | 6.4726 | - | - |
| PGAS | 0.095413 | 0.10116 | 0.28795 | 0.45428 |
| WSTM | 0.52549 | 0.59982 | - | - |
| Sine, 100% | M1 | M2 | M1 | M2 |
| CVGAS | 5.1753 | 5.5628 | 890.19 | 904.79 |
| MASS | 2.3263 | 5.1133 | - | - |
| PGAS | 0.030769 | 0.036145 | 5.0379 | 5.2723 |
| WSTM | 0.18185 | 0.38019 | - | - |
| Sine, 50% | M1 | M2 | M1 | M2 |
| CVGAS | 4.3678 | 4.7659 | 725.15 | 772.07 |
| MASS | 4.3017 | 8.0425 | - | - |
| PGAS | 0.03259 | 0.040114 | 5.698 | 6.5041 |
| WSTM | 0.22628 | 0.47371 | - | - |
| Sine, 0% | M1 | M2 | M3 | M4 |
| CVGAS | 7.8471 | 3.6711 | 646.07 | 256.71 |
| MASS | 33.918 | 45.694 | - | - |
| PGAS | 0.096171 | 0.096003 | 10.515 | 13.677 |
| WSTM | 0.77438 | 0.6574 | - | - |



Fig.6. Control signals at load change test.
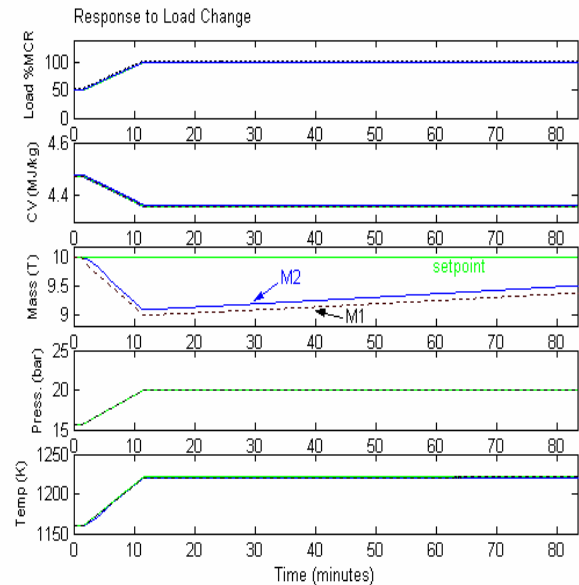


Fig.7. Output signals at load change test

REFERENCES

Al Seyab R. K., Cao Y., and Yang S. H. (2004), A case study of predictive control for the ALSTOM gasifier problem. *Control 2004,* University of Bath, UK.

Dixon R., (1999). Advanced gasifier control. In: *Computing and Control Engineering Journal, IEE,* vol. 10, no. 3, pp. 93-96.

Dixon R., Pike A., and Donne M. (2002). The ALSTOM benchmark challenge on gasifier control. In: *Proc. Instn Mech. Engrs. Part I, Journal of Systems and Control Engineering,* vol. 214, pp. 389-394.

Dixon R., (2002), ALSTOM benchmark challenge II: Control of a non-linear gasifier model. http://www.iee.org/OnComms/PN/controlauto/Specification_v2.pdf

Dumont G., Fu Y., and Lu G. (1994), In: *Advances in model-based predictive control*, Oxford University Press, Oxford.

Rice M., Rossiter J., and Schurmans J. (2002), An advance predictive control approach to the ALSTOM gasifier problem, In: *Proc. Instn Mech. Engrs. Part I, Journal of Systems and Control Engineering,* vol. 13, pp. 759-768.

Sandra A., Norquay J., Palazoglu A., and Romagnoli A. (1998), In: *Chemical Engineering Science*, vol. 53, no. 1 pp. 75-8.